HHS Public Access

Author manuscript

*Am J Ophthalmol*. Author manuscript; available in PMC 2024 July 01.

Published in final edited form as:

*Am J Ophthalmol*. 2024 July ; 263: 188–205. doi:10.1016/j.ajo.2023.11.020.

# Aqueous Humor Liquid Biopsy as a Companion Diagnostic for Retinoblastoma: Implications for Diagnosis, Prognosis, and Therapeutic Options: Five Years of Progress

**JESSE L. BERRY**,
**SARAH PIKE**,
**RACHANA SHAH**,
**MARK W. REID**,
**CHEN-CHING PENG**,
**YINGFEI WANG**,
**VENKATA YELLAPANTULA**,
**JACLYN BIEGEL**,
**PETER KUHN**,
**JAMES HICKS**,
**LIYA XU**

Vision Center, Children's Hospital Los Angeles (J.L.B., S.P., M.W.R., C.-C.P., L.X.); USC Roski Eye Institute, Keck School of Medicine of the University of Southern California (J.L.B., S.P., M.W.R., C.-C.P., L.X.); the Saban Research Institute, Children's Hospital Los Angeles (J.L.B., V.Y., J.B., L.X.); Norris Comprehensive Cancer Center, Keck School of Medicine of the University of Southern California (J.L.B., P.K., J.H.); Cancer and Blood Disease Institute, Children's Hospital Los Angeles (R.S.); Department of Quantitative and Computational Biology, University of Southern California (Y.W.); Center for Personalized Medicine, Children's Hospital Los Angeles

Inquiries to Jesse L. Berry, Children's Hospital Los Angeles, Los Angeles, California, USA; jesse.berrymd@gmail.com.

Author Contributions: Conception and design of the study: J.L.B., P.K., J.H., L.X.; Analysis and interpretation of data: J.L.B., S.P., M.W.R., C.-C.P., Y.W., V.Y., J.B., L.X.; Writing the article: J.L.B., S.P., L.X.; Critical revision of the article: M.W.R., P.K., J.H.; Final approval of manuscript: J.L.B., S.P., R.S., M.W.R., C.-C.P., Y.W., V.Y., J.B., P.K., J.H., L.X.; Data collection: J.L.B., C.-C.P., Y.W., V.Y., L.X.; Provision of patients: J.L.B., R.S.; Statistical expertise: M.W.R.; Obtaining funding: J.L.B.; Literature search: J.L.B., S.P., L.X.; Logistical support: J.B., P.K., J.H.

CREDIT AUTHORSHIP CONTRIBUTION STATEMENT

**Jesse L. Berry:** Conceptualization, Data curation, Formal analysis, Funding acquisition, Investigation, Methodology, Project administration, Resources, Supervision, Validation, Writing – original draft, Writing – review & editing. **Sarah Pike:** Data curation, Writing – original draft. **Rachana Shah:** Conceptualization, Data curation, Formal analysis. **Mark W. Reid:** Data curation, Formal analysis, Writing – original draft, Writing – review & editing. **Chen-Ching Peng:** Data curation, Formal analysis, Writing – original draft. **Yingfei Wang:** Data curation, Formal analysis. **Venkata Yellapantula:** Data curation, Formal analysis, Writing – review & editing. **Jaclyn Biegel:** Data curation, Formal analysis, Writing – review & editing. **Peter Kuhn:** Conceptualization, Data curation, Formal analysis, Writing – review & editing. **James Hicks:** Conceptualization, Data curation, Formal analysis, Writing – review & editing. **Liya Xu:** Conceptualization, Data curation, Formal analysis, Investigation, Methodology, Project administration, Supervision, Validation, Writing – original draft, Writing – review & editing.

Financial Disclosures: J.L.B., L.X., and J.H. have filed a provisional patent entitled Aqueous Humor Cell-Free DNA for Diagnostic and Prognostic Evaluation of Ophthalmic Disease 17/045,435.

The other authors have no conflict of interest to disclose.

All authors attest that they meet the current ICMJE criteria for authorship.

(V.Y., J.B.); USC Michelson Center for Convergent Biosciences and Department of Biological Sciences (P.K., J.H.), Los Angeles, California, USA.

## Abstract

• **PURPOSE:** To define the prospective use of the aqueous humor (AH) as a molecular diagnostic and prognostic liquid biopsy for retinoblastoma (RB).

• **METHODS:** This is a prospective, observational study wherein an AH liquid biopsy is performed at diagnosis and longitudinally through therapy for patients with RB. Tumor-derived cell-free DNA is isolated and sequenced for single nucleotide variant analysis of the *RB1* gene and detection of somatic copy number alterations (SCNAs). The SCNAs are used to determine tumor fraction (TFx). Specific SCNAs, including 6p gain and focal *MycN* gain, along with TFx, are prospectively correlated with intraocular tumor relapse, response to therapy, and globe salvage.

• **RESULTS:** A total of 26 eyes of 21 patients were included with AH taken at diagnosis. Successful ocular salvage was achieved in 19 of 26 (73.1%) eyes. Mutational analysis of 26 AH samples identified 23 pathogenic *RB1* variants and 2 focal *RB1* deletions; variant allele fraction ranged from 30.5% to 100% (median 93.2%). At diagnosis, SCNAs were detectable in 17 of 26 (65.4%) AH samples. Eyes with 6p gain and/or focal *MycN* gain had significantly greater odds of poor therapeutic outcomes (odds ratio = 6.75, 95% CI = 1.06–42.84, $P = .04$). Higher AH TFx was observed in eyes with vitreal progression (TFx = 46.0% ± 40.4) than regression (22.0 ± 29.1; difference: −24.0; $P = .049$).

• **CONCLUSIONS:** Establishing an AH liquid biopsy for RB is aimed at addressing (1) our inability to biopsy tumor tissue and (2) the lack of molecular biomarkers for intraocular prognosis. Current management decisions for RB are made based solely on clinical features without objective molecular testing. This prognostic study shows great promise for using AH as a companion diagnostic. NOTE: Publication of this article is sponsored by the American Ophthalmological Society.

Retinoblastoma (RB) is a childhood cancer of the developing retina and is diagnosed in the first years of a child's life. It is the most common pediatric eye cancer, and it accounts for 3% of all childhood cancers.[1,2] RB can form in one (60%) or both (40%) eyes and is diagnosed in 300 children per year in the United States and 8000 children worldwide. The goals of the treatment are to save the eye and cure the child (with some useful vision). If the tumor is confined to the eye at diagnosis, there is > 99% overall survival rate from this cancer; however, even in high-income countries, ocular survival is far less.[3] Intraocular recurrence after failed attempts at therapy remains quite common, and enucleation is required to prevent extraocular spread in upward of 50% of patients with advanced intraocular disease.[4–7] Unfortunately, there is a poor understanding of the molecular basis underlying the clinical behavior of this cancer. At this time, there are no molecular biomarkers that can prognosticate those eyes that are likely to respond to therapy and be saved and those that are likely to fail therapy and require enucleation to save the child's life. The major reason for this is that we cannot biopsy RB tumors because of the risk of extraocular cancer spread.[8–11]

In terms of cancer genomics, RB is considered a canonical cancer, as *RB1* was the first molecularly described tumor suppressor gene,[12] and chromosomal alterations were shown to drive tumorigenesis.[13] This discovery paved the way for a precision medicine approach across multiple cancer types. Ironically, the cancer that started this field has never benefitted directly from it as a consequence of the contraindication to tumor biopsy. Thus, the majority of genomic studies in RB, which require access to tumor DNA, have been performed only on advanced tumors from surgically removed eyes. Children with RB are not part of the National Cancer Institute-Children's Oncology Group Pediatric MATCH trial, which is intended to molecularly sequence every pediatric malignancy, as there are no clinically available means to attain tumor DNA without eye removal. Because of this, there is no possibility of precision medicine approaches for RB.[14, 15] Currently, the diagnosis and ocular prognosis (the likelihood of saving the eye with therapy) for children with RB are based entirely on clinical examination and imaging due to the lack of in vivo biomarkers. Due to these real-world clinical problems, a liquid biopsy approach, which enables detection of tumor DNA and prognostic molecular biomarkers in the absence of tumor tissue, is critically needed to direct eye salvaging therapies for this cancer.

In 2017, our laboratory demonstrated for the first time that the aqueous humor (AH), the clear fluid in front of the eye, is an enriched source of tumor-derived cell-free DNA (cfDNA) in RB eyes.[16, 17] This breakthrough provided the opportunity to use the AH for the evaluation of tumor-specific biomarkers to support molecular diagnosis and prognosis for RB. These findings opened up a whole new field of research. Over the last 5 years, we have developed a liquid biopsy assay to detect somatic copy number alterations (SCNAs), which are markers of aneuploidy and involve often large regions of chromosomal segments that are gained (too many copies) or lost (too few copies), thus facilitating tumor growth. We can also identify diagnostic pathogenic *RB1* variants from the AH—all from a single 100 μL sample—and the alterations are the same as would be identified in tumor tissue[18–20]—highlighting the ability of the AH to act as a liquid or surrogate biopsy for RB. On the basis of retrospective analysis, we identified potential candidate biomarkers, such as too many copies of chromosomal region 6p (called 6p gain) and focal gain of the *MycN* oncogene, a known poor prognostic biomarker for RB and other cancers. The presence of these biomarkers in the AH was associated with a 16.5-fold increased risk of treatment failure requiring surgical removal of the eye.[21, 22]

We further demonstrated that changes in AH cfDNA tumor fraction (TFx) (ie, the percent of DNA that is tumor derived) correlate with tumor response to treatment, with increases in TFx being indicative of residual intraocular disease that portends cancer relapse within the eye, requiring enucleation.[23] Using the AH liquid biopsy, we most recently investigated the genome-wide methylation status of 850,000 separate loci to identify genes aberrantly activated or inactivated via epigenetic mechanisms.[24] With the ability to profile gene methylation status in vivo via the AH, we were able to identify low- and high-risk subtypes of RB, which were highly concordant with RB subtypes determined through studies that analyzed tumor tissue from enucleated eyes.[25] Finally, as nearly 40% of children with RB have cancer in both eyes, and each eye often presents with distinct genomic alterations,[26] an eye-specific liquid biopsy to direct ocular prognosis and therapy has potential to be highly beneficial.[27]

Although our laboratory led the research in this arena,[16] we were quickly joined by centers around the world studying a liquid biopsy for RB.[28] Most of this work has involved validating our discovery regarding the presence of tumor DNA in the AH by identifying the presence of *RB1* mutant DNA (for molecular diagnosis of RB).[29–32] A few centers have investigated prognostic AH biomarkers including survivin,[33] metabolomic signatures,[34] and expression of secreted peptides.[35] Other centers are also evaluating SCNAs and their impact on RB ocular prognosis.[36] However, the majority of these studies, including our own, are retrospective and use AH samples taken only midtreatment or at the time of enucleation. It was not known what, if any, biomarkers were present in the AH at diagnosis, and whether they mattered. Because of the potential clinical impact of this liquid biopsy, we developed a prospective approach that includes AH taken at the time of diagnosis from eyes with the intent to salvage (ie, not at the time of primary enucleation). The goal of prospective biomarker validation, as opposed to all previous retrospective reports, is to understand if the biomarker is (1) detectable at diagnosis and (2) whether it does indeed prognosticate outcomes when identified at diagnosis. This is currently unknown for RB and must be answered before the broader ocular oncology community can use these results clinically. An initial prognostic report of the first 12 months of data has been published.[22] Herein we will present data from 26 separate consecutive eyes with RB, with extended follow-up and AH sampling, with the ultimate goal of biomarker validation for RB.

In this paper we aim to establish, based on prospective evaluation, that (1) cfDNA biomarkers identifiable at diagnosis are associated with aggressive intraocular tumor behavior; (2) tumor-derived *RB1* mutation(s) are detectable in the AH routinely, which can impact clinical genetic testing and counseling; and (3) monitoring of TFx in the AH is a distinct molecular biomarker that correlates with treatment outcomes. We assert that the ability to prognosticate ocular outcomes via the AH will help identify patients with eyes that are likely to be saved, as well as those with eyes more likely to fail treatment and require removal. This has the potential to help ocular oncologists and parents make informed treatment choices based on the available molecular biology of the time and hopefully in the future open new, impactful personalized medicine approaches to this eye cancer.

## METHODS

### • PATIENT, SAMPLE, AND MULTISITE CHARACTERISTICS:

Study participants include patients diagnosed with RB at Children’s Hospital Los Angeles (CHLA). Research is performed under an established, prospective institutional review board–approved Retinoblastoma Patient Clinical Database and Tissue Biorepository. Biospecimens with associated coded clinical data are collected. Children with bilateral disease can contribute samples and clinical data from both eyes. Eye classification for RB ranges from International Intraocular Retinoblastoma Classification (IIRC)[37] groups A-E, with E being the most advanced; group A eyes have tumors < 3 mm. Clinical outcomes (eg, globe salvage or enucleation) are evaluated with at least 12-month follow-up. The treatment for all patients is carried out per routine clinical protocol, which may include either systemic or intra-arterial chemotherapy for primary eye salvage, followed by intravitreal injections of chemotherapy as needed.[6, 38, 39] AH genomic testing results did not influence treatment.

Not all treatments will be required for each child, and only some children will have intraocular recurrences or enucleation; thus, there are a range of AH samples collected depending on the child's clinical course.

### • SPECIMEN COLLECTION AND STORAGE:

Specimen collection and storage has been described in depth.[40] In brief, all samples are taken while the child is under anesthesia for routine clinical care. No child was placed under anesthesia for research purposes. A clear corneal paracentesis[40] with a 32-gauge needle is performed to extract up to 100 μL of AH from RB eyes. AH extraction is taken at diagnosis, at the end of chemotherapy and 6 months from the end of therapy, during intravitreal injections for seeding (if required), and at the time of a recurrence or immediately after enucleation of the eye (if these events occur). If an enucleation is required to save the child from progressive disease, tumor tissue is obtained. During sampling, needles enter only the anterior chamber via the clear cornea and remain bevel-up over the pharmacologically dilated iris; thus, they do not touch the iris, lens, vitreous cavity, or tumor. Although the anterior chamber may shallow slightly, it remains formed. Immediately after specimen extraction, AH samples are flash-frozen on dry ice and quickly stored at −80 °C within hours of extraction.

### • AQUEOUS HUMOR CELL-FREE DNA ISOLATION AND LIBRARY CONSTRUCTION:

CfDNA from AH and blood plasma is isolated with the QIAamp Circulating Nucleic Acid Kit (Qiagen). Library construction and sequencing of cfDNA have been described in detail.[40–42] Briefly, isolated cfDNA is constructed into whole genome libraries using the QIAseq Ultralow Input Library Kit (Qiagen). The same library created from the AH cfDNA is used for *RB1* mutation analyses and genomic analyses.

### • DETECTION OF PATHOGENIC SOMATIC RB1 VARIANTS FOR MOLECULAR DIAGNOSIS (SINGLE-NUCLEOTIDE VARIANTS):

Mutation detection is done using a customized laboratory-developed hybridization panel (Cancer Predisposition Panel; Twist Bioscience), based on our published data for AH, using a SureSelect panel (Agilent).[20] This panel covers > 500 cancer predisposition genes, including the whole exonic regions of the *RB1* gene, *MycN* gene, and lesser-known implicated genes such as *BCOR, ARID1A*, and *CREBBP*. Illumina sequencing is carried out on the captured libraries. Bioinformatics analysis is performed to characterize single-nucleotide variant (SNV) and loss of heterozygosity detection using an in-house pipeline in collaboration with the CHLA Center for Personalized Medicine.

### • WHOLE GENOME SOMATIC COPY NUMBER PROFILING OF AQUEOUS HUMOR SAMPLES FOR MOLECULAR PROGNOSIS (SCNAS):

Analysis of the cfDNA from AH samples is based on established methods of SCNA analysis.[40–42] Briefly, whole genome libraries are sequenced on an Illumina HiSeq (Illumina) platform. Copy number values are recorded as ratios to the median (relative to a baseline human genome), with values ≤0.87 representing copy number losses and values ≥1.15 representing copy number gains equal to 20% deflection from the human genome; due

to tumor heterogeneity in a non–single-cell approach, values within 0.01 of these thresholds were considered positive, for example, values ≤0.86 representing copy number losses and values ≥1.14 representing copy number gains.

- **DETERMINATION OF CELL-FREE DNA TUMOR FRACTION IN THE AQUEOUS HUMOR:**

The cfDNA TFx for each sequenced AH cfDNA sample is estimated using the ichorCNA software (https://github.com), a standard validated tool for TFx assessment.[43] The algorithm employed by ichorCNA to determine TFx in the serum has been described in detail.[43, 44] In short, ichorCNA uses a hidden Markov model to predict large-scale SCNAs within sequenced cfDNA. TFx estimations are thus based on the presence of SCNAs while accounting for differences in ploidy and subclonality at each locus. An optimal TFx solution is provided by ichorCNA.[43] The TFx is correlated with the actual SCNA amplitude generated from our genome sequencing protocol; higher TFx has been shown to correlate with higher SCNA amplitudes, which can be used as a surrogate to TFx values.

- **CORRELATION OF TUMOR FRACTION AND CLINICAL OUTCOMES:**

Based on examinations under anesthesia, the therapeutic response of the tumor at the time of each AH extraction is recorded as either progressing, regressing, or stable disease using the established RB-RECIST guidelines.[45] We longitudinally evaluated cfDNA TFx in the AH to determine objective thresholds for treatment response at the end of primary therapy and thresholds that indicate minimal residual intraocular disease.

- **DEMOGRAPHICS AND CLINICAL DATA:**

To assess the relationship between the identified molecular biomarkers and clinical features of RB, 89 unique clinical data points are recorded into the institutional review board–approved biorepository from each patient and eye(s), including age at diagnosis, sex, laterality, IIRC group/tumor, nodes, metastases staging,[46, 47] seeding morphology, therapies given at each stage, histopathology, and follow-up times. RECIST guidelines, which stand for Response Evaluation Criteria in Solid Tumors, is the standard accepted methodology in oncology to evaluate tumor outcomes. Herein, treatment outcomes (eg, tumor response, recurrence, ultimate globe salvage, and metastatic disease) are obtained according to the specific guidelines published for RB, called RB-RECIST.[45] Data are coded when entered in the biorepository database.

- **STATISTICAL CONSIDERATIONS:**

Logistic regression was used to evaluate whether previously identified biomarker candidates, 6p gain and focal *MycN* gain, are prognostic for poor therapeutic outcomes (recurrence or enucleation) in the prospective data set. Second, time to outcome (eg, time to recurrence or enucleation) was evaluated with a Cox proportional hazard model. Because of limited study power, both models evaluated the biomarker without covariates. To examine the impact of covariates on results, 2 additional subanalyses were conducted on each model using 3 covariates—age at diagnosis, sex, and IIRC group; in the first subanalysis, the effects of covariates on the prognostic utility of the biomarker were considered, and in the second

subanalysis, the effects of covariates adjusted to be uncorrelated with the biomarker, but related to the outcome, were considered.

TFx is reported as whole percentages instead of decimal values (eg, 27% instead of 0.27) and is summarized as mean ± SD throughout. To account for the non-normal distribution of TFx data, values were compared between groups using Mann-Whitney *U* tests. Longitudinal data from all SCNA or *RB1* positive eyes that have more than 1 AH sample collected were evaluated to determine the clinical utility of cfDNA TFx for predicting treatment response; as the change in TFx between samples is as important as (or possibly even more than) a single value, we included only eyes with more than 1 AH sample taken longitudinally during treatment. The lowest limit of detection for tumor DNA in the sample is 10%, which is a widely accepted cutoff for iChor analysis although lower reads are available.[48, 49] Therefore, patients with longitudinal samples who had < 10% TFx by SCNAs in their diagnostic AH sample were excluded from longitudinal analyses regardless of the total sample number. Each eye may contribute a different number of AH samples, depending on treatment requirements during the study. We considered TFx, and the change in TFx, in longitudinal AH samples compared with the initial sample. Analysis consisted of logistic regression models evaluating TFx as a predictor of clinical response (progression or regression) in samples collected during therapy, one using TFx as a continuous measure (0%−100%) and the second replicating the 15% cutoff values described in the paper by Polski and associates[23] (ie, the % change in TFx between samples, or the % change relative to baseline).

## RESULTS

### • PARTICIPANT DEMOGRAPHICS AND CLINICAL OUTCOMES:

A total of 26 eyes of 21 patients were included in the study; this includes 3 IIRC group A eyes, 2 group B eyes, 4 group C eyes, 16 group D eyes, and 1 group E eye. Cases 44, 70, 72, 74, and 88 presented with bilateral disease and both eyes were included. Demographics, diagnostic clinical features, and therapeutic courses are summarized in Table 1. Treatment courses for eye salvage were nonrandomized and decided by the treating physicians without prior knowledge of the AH biomarkers; case 65 was enrolled in the study with AH taken at diagnosis and plan for salvage therapy; however, the family decided a week later to pursue primary enucleation. No patients had complications secondary to AH sampling, including infection, iris trauma, synechiae, hyphema, or cataract. Successful ocular salvage was achieved in 19 of 26 (73%) eyes with 7 requiring enucleation. No child developed extraocular disease or metastatic disease throughout the follow-up period. No participants included in this study withdrew consent or were lost to follow-up over the study period. Average follow-up was 33 months (range: 12–56 months).

### • AQUEOUS HUMOR LIQUID BIOPSY: DIAGNOSTIC CONCENTRATION AND RB1 PATHOGENIC VARIANTS:

Of the 26 AH samples, 23 were available for cfDNA quantification, due to the volume of AH needed for analyses. cfDNA was detectable in 19 (82.6%) of these samples (mean

double-stranded DNA concentration 8.8 ng/μL, SD 16.6 ng/μL, median 1.1 ng/μL, range 0.076–56.6 ng/μL) (Table 2).

The AH sample at diagnosis was evaluated for detection of *RB1* pathogenic variants. Mutational analysis of 26 AH samples identified 23 pathogenic *RB1* somatic variants and 2 *RB1* deletions in 19 samples (73.1%). The variant allele fraction (VAF) of the mutated gene ranged from 30.5% to 100%, with a median of 93.2% and a mean of 72.8% (Table 2). As per standard, the VAF is calculated as the number of altered or "variant" reads over the total reads (altered and nonaltered). Mutational analysis did not identify either an *RB1* pathogenic variant or deletion in 7 eyes, 4 from IIRC group A or B eyes with small tumors. Of more advanced group C, D, and E eyes, mutational analysis was successful in 18 of 21 (85.7%) eyes. Case 48 is one case wherein an *RB1* variant was not detected; this case also demonstrated a focal *MycN* gain.[50–53] Tumor tissue was available for this case due to enucleation; *RB1* variants were also not detected.

## • AQUEOUS HUMOR LIQUID BIOPSY: DIAGNOSTIC SCNAS:

AH cfDNA at diagnosis was evaluated via low-pass whole-genome sequencing (WGS) for the presence of highly recurrent RB SCNAs including gain of 1q, 2p, 6p, loss of 13q, 16q, focal *MycN* gain, and focal *RB1* deletion (identified on low-pass WGS). SCNAs were detectable in 17 of 26 (65.4%) AH samples from eyes with RB ranging from group A to E at diagnosis. Among the 17 eyes with positive SCNAs present in their diagnostic samples, none were classified as IIRC group A, 1 (5.9%) was group B, 2 (11.7%) were group C, 14 (82.4%) were group D, and none were group E (Table 3, Figure 1). Nine of the 26 eyes (34.6%) had no identified SCNAs at diagnosis, including group A and E eyes. This is concordant with past reports,[19] suggesting that approximately two-thirds of RB tumor samples from enucleated eyes have SCNAs. This included the presence of focal *RB1* gene deletions, which was seen in cases 44_OS and 64. As with the *RB1* alterations, a lower concentration of cfDNA due to small tumor size can affect this WGS analysis. Thus, excluding group A and B eyes, SCNAs were identified in 16 of 21 (76.2%) eyes and 14 of 16 (87.5%) of group D eyes demonstrating the overall stability of this value, and also that not all eyes, even advanced eyes, will have SCNAs.

Of the highly recurrent RB-SCNAs, 1q gain was present in 13 of 26 eyes (50.0%), 2p gain in 5 of 26 eyes (19.2%), 6p gain in 11 of 26 eyes (42.3%), 13q loss in 1 of 26 eyes (3.8%), 16q loss in 7 of 26 eyes (26.9%), and focal *MycN* and *MDM4* gain seen in 1 eye each (3.8%) (Figure 2).

## • AQUEOUS HUMOR LIQUID BIOPSY: PROGNOSTICS FOR INTRAOCULAR RECURRENCE:

All eyes were followed longitudinally throughout therapy for at least 12 months (median follow-up: 33 months).

An intraocular recurrence was detected in 14 of 26 eyes (53.8%), including 4 eyes with a retinal recurrence, 9 eyes with a seeding recurrence, and 1 eye with both. Overall, 19 of the 26 eyes (73.1%) were cured with therapy and 7 (26.9%) required enucleation. Case 65 was enrolled in the study with plans for salvage, and the family subsequently decided to pursue primary enucleation; the other 6 eyes (cases 33, 48, 55, 66, 67, and

72_OS) required secondary enucleation as definitive management due to persistently active intraocular disease. Thus, 19 of 25 eyes (76%) that underwent salvage were cured, and 6 of 25 (24%) failed globe conservation attempts.

The subset of eyes with more “aggressive” tumor behavior was defined by recurrent ocular disease and/or the need for enucleation. We evaluated the 15 eyes with an intraocular relapse and/or enucleation for the presence of 6p gain or a focal *MycN* gain present at diagnosis, which have been previously identified as poor prognostic factors for overall globe salvage.[50 , 54] Nine of these 15 eyes demonstrated 6p gain and/or focal *MycN* gain (60%) in the AH liquid biopsy at diagnosis. Eleven eyes did not have an intraocular relapse (neither seeding, nor retinal recurrence) and were saved with therapy; of these, only 2 (18.2%) demonstrated 6p gain and/or *MycN* gain (cases 51 and 74_OS) (Table 1, Figure 1).

In a logistic regression model predicting either recurrence or enucleation, eyes from patients with 6p gain and/or focal *MycN* gain (n = 11) had significantly greater odds of poor therapeutic outcomes (odds ratio [OR] = 6.75, 95% CI = 1.06–42.84, $P = .04$). When time to recurrence or enucleation was considered in a Cox proportional hazard model, those with 6p gain and/or *MycN* gain had significantly greater hazard of recurrence or enucleation (hazard ratio = 3.12, 95% CI = 1.10–8.81, $P = .03$, see Figure 3).

By IIRC class, the most robust data are for the 16 group D eyes included in this study. Of these 16 eyes, 12 (75%) demonstrated aggressive tumor behavior. Of these 12 eyes, 8 (66.7%) had 6p gain compared with 6p gain in just 1 of the 4 eyes (25%) that did not demonstrate an intraocular recurrence and were saved (case 51).

## • AQUEOUS HUMOR LIQUID BIOPSY: TUMOR FRACTION AS A PREDICTOR OF DISEASE PROGRESSION:

All diagnostic AH samples were analyzed for TFx using the iChor software (Table 4). iChor relies on the presence of SCNAs to determine TFx. Thus, 8 of the 26 eyes (30.7%) had no/few SCNAs and thus TFx values below the 10% threshold (cases 44_OD, 44_OS, 46, 64, 70_OS, 84, 88_OD, and 88_OS). In cases 44_OD and 64, a somatic *RB1* deletion was detected in the AH, but no other SCNAs detected (Figure 2).

Although iChor determined the TFx to be < 10% due to the absence of SCNAs, *RB1* mutational analysis did demonstrate tumor DNA with high TFx in many of these cases (cases 44_OD, 44_OS, 46, 88_OD, and 88_OS), highlighting the benefit of detecting tumor DNA via more than 1 mechanism.

Of the 18 eyes with greater than 10% TFx in their diagnostic AH sample, 11 had 2 or more AH samples collected, allowing for longitudinal analysis (Table 4). The TFx values in those eyes *responsive* to RB treatment showed a trend of decreased TFx value compared with the DX sample, whereas the TFx values of those eyes *resistant* to treatment maintained high TFx values similar to the diagnostic sample. Seven of the 11 eyes (cases 47, 51, 73, 74_OD, 74_OS, 76, and 78) were salvaged with treatment, and their TFx trends reflect this; in addition, the final samples on all of these cases were < 10% TFx with the exception of case 51, which was 11.1% at the end of therapy. TFx values remain longitudinally elevated

in cases 33 and 55, suggesting treatment resistance—both of these eyes were secondarily enucleated after treatment failure. Case 67 was an outlier that had a relatively low TFx at the time of secondary enucleation (3.1%); this case was treated with 1 cycle of intra-arterial chemotherapy, and there remained no view to posterior pole, so the decision was made to enucleate; histopathology showed near complete tumor necrosis.

TFx at diagnosis, as well as the change in TFx seen between subsequent samples, was used to characterize disease progression and regression. In general, higher AH TFx was observed in eyes with vitreal progression (TFx = 46.0% ± 40.4%) than regression (22.0% ± 29.1%; difference: −24.0; $P = .049$). In samples where retinal progression had occurred, the same general pattern was observed, where progression was associated with higher TFx values (38.2% ± 40.4%), and regression was associated with lower values (24.4% ± 30.9%), but the difference was not statistically significant ($P = .44$).

When used as a predictor of vitreal progression in a logistic regression model adjusted for age, sex, and presence of 6p gain or *MycN*, each 1% increase in baseline TFx was associated with 1.03 times greater odds of progression (OR = 1.03, 95% CI = 1.002–1.05, $P = .03$). Baseline TFx was not significantly associated with increased odds of retinal progression, although the magnitude of the effect is similar (OR = 1.01, 95% CI = 0.99–1.03; $P = .29$).

Changes in TFx in a given sample relative to previous TFx samples were also evaluated in cases where multiple samples were obtained using logistic regression models. In general, changes in TFx relative to the previously obtained sample did not predict progression. However, changes in TFx relative to baseline showed nonsignificant trends in the expected direction (eg, for retinal progression, OR = 1.04, 95% CI = 0.99–1.08, $P = .10$). TFx changes reduced to a 15% cutoff, as described in the paper by Polski and associates,[23] could not be evaluated as there were too few changes of this magnitude in the current data.

### • CONCORDANCE WITH MATCHED TUMOR:

Of the 26 eyes in the study, 7 were enucleated. Tumor tissue was available for analysis from 6 of 7 eyes; 1 eye (case 67) was enucleated at an outside hospital while the primary surgeon was on maternity leave.

When tumor was available, concordance was determined by dividing the median segmented ratio values for the tumor by the median segmented ratio values for the AH and calculating the percentage of “bins” in which the ratio was within 0.8 to 1.2 (excluding chromosomes X and Y).[55] In genomic testing, grouping reads to “bins” means aligning and assigning them to regions of the genome. As per previous reports,[18] AH tumor pairs were 96.6% concordant (range, 92.8%−98.7%)

## DISCUSSION

### • WHERE HAVE WE COME FROM?:

In 2017, the first report of using the AH as a liquid biopsy to serve as a surrogate to tumor biopsy for RB was published.[16] For the first time ever, tumor-derived DNA and other tumor-derived molecules were safely available in vivo from an eye with RB that had not

been enucleated. This ushered in an exciting new era of liquid biopsy research[17] and began the search for actionable liquid biopsy biomarkers for ocular tumors.[56]

Only approximately 5 years have passed from this initial report, and in the interim, we have identified some important biomarkers suggesting the clinical utility of AH analysis for children with RB. First, with the ability to compare genomic profiles from eyes that respond to therapy, and those that fail therapy, we noted that there seemed to be a disparity in both the incidence and the amplitude of the known highly recurrent RB SCNA, gain of chromosome 6p. In fact, in our 2018 report,[18] which was the first study to correlate clinical outcomes with SCNAs in the AH from RB eyes, we found that gain of chromosome 6p was the most common SCNA in RB AH. With AH samples taken during therapy, this alteration was found in 77% of enucleated eyes, compared with 25% of salvaged eyes ($P = .0092$), and associated with a 10-fold increased odds of enucleation (OR = 10, 95% CI: 1.8–55.6). The median amplitude of 6p gain was 1.47 in enucleated vs 1.07 in salvaged eyes ($P = .001$). Overall, the presence of AH SCNAs, which indicates increased genomic instability, was correlated retrospectively with eye salvage. The probability of ocular salvage was significantly higher in eyes without detectable SCNAs in the AH ($P = .0028$), specifically 6p gain. Thus, these findings indicated that 6p gain in the AH was a potential prognostic biomarker for poor clinical response to therapy.[18]

We continued to evaluate the AH in an effort to better understand the genomic landscape of RB tumors in vivo. This research led to a few exciting conclusions. First, we were able to re-evaluate the findings of past studies that only had genomic information available from tumor tissue obtained from enucleated eyes—arguably from the most advanced and aggressive tumors. In an analysis of AH sampled from 54 eyes of 50 patients, we compared overall genomic instability (number of SCNAs) to RB1 status, IIRC group, and age.[54] Previous reports had suggested that patients without germline *RB1* mutations were more likely than patients with germline mutations to develop genomic instability.[57] However, in that study, there was a significant association between younger age and germline disease. Of the 50 patients in evaluated cohort, 23 (46.0%; 27 eyes) had hereditary RB and 27 (54.0%; 27 eyes) had nonhereditary RB. Median age at diagnosis was comparable between hereditary (13 ± 10 months) and nonhereditary (13 ± 8 months) RB patients ($P = .818$). There was no significant difference in the prevalence or number of SCNAs based on (1) hereditary status ($P > .56$) or (2) IIRC grouping ($P > .47$). There was, however, were significant correlations between patient age at diagnosis and (1) number of total SCNAs ($r(52) = 0.672$, $P < .00001$) and (2) number of highly recurrent RB SCNAs ($r(52) = 0.616$, $P < .00001$). This evidence does not support the theory that specific molecular or genomic subtypes exist between hereditary and nonhereditary RB; rather, the prevalence of genomic alterations in RB eyes is strongly related to patient age at diagnosis with older children having more intratumoral genomic instability regardless of *RB1* germline status.

Ongoing comprehensive genomic analyses of RB in vivo facilitated by the AH liquid biopsy demonstrated that, as with other cancers, genomic instability was associated with more aggressive disease.[19] We found that increases in chromosomal instability were associated with more advanced seeding morphology (ie, cloud vs sphere vs dust, $P = .015$), later age of diagnosis ($P < .0001$), greater odds of an endophytic tumor growth pattern (without

retinal detachment, $P = .047$), and larger tumor sizes with heights > 10 mm ($P = .09$). We also identified some less commonly seen alterations, such as 20q gain and 8p loss, which differed between primarily and secondarily enucleated eyes—including changes in genomic alterations that were detected in the AH under therapeutic pressure.

Although overall genomic instability appeared to be a poor prognostic biomarker, the evidence continues to mount for 6p gain as a useful and powerful predictor of significant intraocular tumor recurrence, most often leading to secondary enucleation due to treatment resistance. In a 2020 study published in *Molecular Cancer Research*, with nearly twice the number of eyes and length of follow-up, we continued to demonstrate with our findings that 6p gain was a potential prognostic biomarker for aggressive tumor behavior for RB.[21] Again, 6p gain was the most prevalent SCNA (50% eyes). It was particularly more prevalent in enucleated eyes (73.9%) than in salvaged eyes (29.6%; $P = .004$). 6p gain in AH cfDNA portended nearly 10-fold increased odds of enucleation (OR = 9.87, 95% CI = 1.75–55.65, $P = .009$). In the enucleated eyes, 6p gain was associated with aggressive histopathologic features, including necrosis, higher degrees of anaplasia, and focal invasion of ocular structures. Other researchers similarly investigated 6p as a marker for aggressive RB and found that it was associated with severe anaplasia in tumor specimens, significant and quantifiable changes in tumor staining characteristics, and most concerning, with extraocular tumor spread.[58]

This highly recurrent alteration was not discovered via the AH liquid biopsy. Rather, 6p gain had long been hypothesized to play a role in RB tumorigenesis beyond loss of *RB1*.[13] We and others have shown that 6p gains often span the entire region of 6p—consistent with the formation of an isochromosome, in which misdivision at the centromere leads to abnormal gain of the entire 6p arm in the tumor.[59] This isochromosome is the most common underlying cause of 6p gain in RB and is unique—it is rarely seen in other ocular malignancies.[59] Previous studies of tumor tissue have identified the common region of 6p gain to 6p22, a central region of the short arm of chromosome 6 that contains numerous genes.[13, 59–61] The oncogenes *DEK* and *E2F3* have been hypothesized to be the most likely drivers of RB in this region, as they demonstrate both RNA and protein overexpression in the setting of 6p gains and promote abnormal cell proliferation when overexpressed.[13, 59, 62] We also found that *E2F3* and *DEK* are almost always included within the region of 6p gain, regardless of the width of the alteration. Although *DEK* and *E2F3* remain promising RB candidate genes, 6p gains are highly nonfocal in nature and include hundreds of different genes in addition to *DEK* and *E2F3*— making it difficult to distinguish between true driver genes in this region vs passenger events.[13, 61, 63] It remains unclear whether a particular gene (or genes) on 6p is driving aggressive tumor activity, or whether 6p gain is simply a measurable molecular marker of other underlying processes within the tumor genome.

- **WHERE ARE WE?:**

The data herein represent the first 26 eyes of 21 patients included in prospective, longitudinal analysis of the AH liquid biopsy. Tumor-derived cfDNA from the AH was isolated at diagnosis for complete genomic analysis to include SCNAs, *RB1* mutational analysis, and TFx, which was evaluated longitudinally.

In terms of diagnosis, this AH platform detected 23 pathogenic *RB1* somatic variants and 2 focal *RB1* deletions in 19 of 26 samples (73.1%) with a median VAF of 93.2% (range, 30.5%−100%) (Table 2). Excluding small tumors with low DNA concentration (groups A and B, < 3 mm tumors), mutational analysis was successful in 18 of 21 (85.7%) eyes. Although approximately 85% is consistent with rates of mutation detection in the literature,[53, 64] there are multiple reasons why a mutation may not be detected in the AH. This includes low quantity of DNA input, difficulty with probes annealing to cfDNA, particularly in exonic reasons, or that a mutation is not actually present and rather oncogenesis is due to epigenetic dysregulation via methylation of the promotor, which is a known driver of RB tumorigenesis in the absence of an *RB1* mutation.[65, 66] This would not be identified by our current assay (but is planned for future versions). Another possibility is that a tumor is driven by *MycN* amplification with intact *RB1*; focal *MycN* gain is routinely detected via our SCNA assay, thus providing multiple levels of molecular tumoral information.

Among our cohort, SCNAs were identified in 17 of 26 eyes (65.4%). Not surprisingly, SCNAs were absent in all group A eyes but were identified in 1 group B eye, 2 of the 4 group C eyes, and 14 of the 16 group D eyes (Table 3, Figure 2). SCNAs were also absent in the 1 group E eye included in analysis (88_OD); this patient with bilateral disease was germline *RB1* mutation positive. Our diagnostic cohort exhibited more chromosomal instability in samples from eyes with more advanced disease by IIRC, as previously described.[19] Of the highly recurrent RB-SCNAs, 1q gain was present in 13 of 26 eyes (50.0%), 2p gain in 5 of 26 eyes (19.2%), 6p gain in 11 of 26 eyes (42.3%), 13q loss in 1 of 26 eyes (3.8%), 16q loss in 7 of 26 eyes (26.9%), and focal *MycN* and *MDM4* gain seen in 1 eye each (3.8%).

In this prospective cohort with a median follow-up time of 33 months, we again demonstrate that the presence of 6p gain and/or *MycN* gain was prognostic for intraocular recurrence. Not surprisingly, the most robust data are for the group D eyes—which are also the most commonly seen eyes across most US centers and the most common included in this study. Of the group D eyes, 75% demonstrated aggressive tumor behavior, of which 66.7% had 6p gain in the AH at diagnosis. This is compared with 6p gain in only 1 of the group D eyes that did not demonstrate an intraocular recurrence and were saved (case 51) (Table 3). Overall, in this prospective validation study, 6p gain was associated with increased odds of recurrence or enucleation over time (hazard ratio = 2.95, 95% CI = 1.05–8.34, $P = .04$).

By iChor analysis, 18 eyes in our cohort had diagnostic TFx values greater than the 10% threshold. All of the 7 eyes with the diagnostic TFx value below 10% were negative for whole genome instability, that is, the presence of multiple SCNAs. Five eyes (cases 44_OD, 44_OS, 46, 88_OD, and 88_OS) had high *RB1* gene SNV VAF, which is a surrogate of TFx. However, due to the lack of SCNAs in the diagnostic AH sample, TFx values were < 5% (Table 4, Figure 1). This underscores the need for TFx testing that uses both SCNAs and *RB1* SNV; however, as the concentration of cfDNA decreases in AH samples during treatment (compared with diagnosis), mutation analysis is more technically difficult. Of the eyes with > 10% TFx based on the presence of SCNAs, longitudinal TFx demonstrated a trend of decreasing TFx in those eye responsive to treatment, with persistence of TFx values

similar to the diagnostic sample in eyes nonresponsive to treatment. This is illustrated best in comparing 2 cases. In case 33, the TFx value at diagnosis was 97.0%, and throughout treatment, the TFx remained elevated at > 90%—this eye was ultimately enucleated after treatment failure. In case 73, the diagnostic TFx was 41.8%, and the TFx remained approximately 40% throughout intravitreal chemotherapy with melphalan injection numbers 1 through 4 (A-D), which occurred concurrently with systemic chemotherapy (carboplatin, etoposide, vincristine (CEV)) cycles 2–6 due to persistent intraocular seeding. After 6 cycles of CEV, intravitreal injections with a combination of melphalan and topotecan were initiated (sample F) due to persistent active clinical seeds. Comparing TFx values in the sample taken immediately before mel/topo injection number 1 (sample F) and TFx in a sample taken immediately before mel/topo injection number 2 (sample G), there is a significant drop in TFx, from 55.6% to 6.0%. This correlated with clinical clearance of the active seeds. The patient's TFx value continued to decline and was ultimately 0.0% in the most recent sample collected. This initial lack of decline in TFx correlated with a period of persistent disease while the stark TFx value drop reflected the eye's excellent response to mel/topo therapy, and the subsequent decreasing TFx value trend supports the eye's ultimate treatment salvage. Diagnostic TFx values > 40% were associated with seeding recurrence ($P = .04$), which suggests that these eyes may benefit from intravitreal chemotherapy; however, more samples are needed for robust logistic regression analysis. In addition, there is a trend toward significance both for a TFx at diagnosis > 40% being associated with aggressive disease and for a TFx < 10% at the end of therapy associated with the complete therapeutic effect. TFx was more predictive of vitreal disease progression rather than retinal; however, a trend toward significance was also seen for retinal disease. It may be that vitreous disease is easier to detect via the AH, or simply that this analysis is limited by sample size. Further prospective validation is required before clinical implementation of AH TFx in the care of patients with RB.

Five patients enrolled in this study had a germline pathogenic variant in the *RB1* gene and presented with bilateral involvement of RB. Unlike blood, cerebrospinal fluid, or other liquid biopsy sources of tumor-derived molecular information, the aqueous is specific to the overall tumor state in each eye.[26] This is particularly impactful for patients with bilateral disease. The overall high TFx in the AH also facilitates deep tumoral analysis of both SCNAs and *RB1* SNVs, or deletions. The simple goal to molecularly define solid tumors can be impactful.

- **WHERE ARE WE GOING?:**

From our research, we suggest that the quantity of 6p chromosomal gains in AH may correlate with RB disease severity. This is similar to uveal melanoma (UM), the most common intraocular cancer of adults, where increased copy number (ie, higher amplitude of gain) of chromosome 8q is significantly associated with a worse prognosis.[67] In UM, a gain of 1 copy of chromosome 8q correlates with moderate metastatic risk, whereas higher amplitude of gain is increasingly associated with worse clinical outcomes. It has been proposed that in molecular prognostication of UM, there is a role for chromosome 8q quantification; 8q copy number is even used to classify most severe UM disease by the

Cancer Genome Atlas guidelines.[68] Similarly, we propose a future role for 6p quantification in AH samples for RB disease stratification.

Along with 6p, other biomarkers emerged through AH liquid biopsy analyses. *MycN* amplification is another known marker of aggressive tumor activity, specifically described (from tumor tissue) to initiate RB without loss of the RB protein (*RB1* + / +) and usually seen in young infants with unilateral disease.[50] In our analyses of AH, we identified *MycN* gain both in the setting of intact *RB1* and with *RB1* loss. Regardless of the *RB1* status, *MYCN* was associated with aggressive behavior.[22]

On the basis of extended prospective evaluation of our data,[21] we continue to demonstrate an impactful genomic signature for the risk of intraocular relapse that includes the presence of either 6p gain and/or focal *MycN* gain. This signature is prognostic for a 16.8-fold increased likelihood of treatment failure requiring enucleation. This model is 85.7% sensitive and 73.7% specific for the prediction of intraocular disease recurrence; the positive and negative predictive values are 54.6% and 93.3%, respectively ($P = .02$); this is similar to past data on this model.[22]

With these data, we now have a clinically available, college of american pathologists (CAP)-clinical laboratory improvement amendments (CLIA) laboratory–validated assay available from the Center for Personalized Medicine at CHLA demonstrating the clinical feasibility of combined targeted and WGS of tumors using a liquid biopsy approach in pediatric solid tumors.[69] We hope that the use of this assay will allow for continued molecular characterization of this tumor. This is the basis for the National Cancer Institute Pediatric MATCH trial, to better understand the molecular landscape of pediatric solid tumors, as well as the potential actionable alterations for personalized therapies.[70, 71] In all likelihood, further prospective analysis of the AH will support a similar goal for patients with RB. An improved understanding of biomarkers that impact the care of children with RB, such as 6p and *MYCN* but also *MDM2/4, BCOR* and other genomic alterations that may be impactful to a personalized medicine approach. Prospective, longitudinal analysis may also be impactful to our understanding of treatment resistance. For example, 19q loss has been noted more frequently in secondarily enucleated eyes that have failed therapy.[19, 72] The AH liquid biopsy clinical test, which is now routinely available (https://www.chla.org/center-personalized-medicine), may also be useful in the setting of diagnostic uncertainty such as when there has been loss of view to the fundus.

Outside of genetics and genomics, the AH liquid biopsy platform is poised to identify and define other molecular markers for RB such as methylation signatures,[24, 25, 73] proteomics,[74] and extracellular vesicles.[75] In addition, AH liquid biopsy plays a role in disease diagnosis and prognostication outside of RB. Various analytes present in the AH have been investigated for other ocular cancers including UM[76, 77] and vitreoretinal lymphoma,[78] as well as for nononcologic ocular diseases such as age-related macular degeneration,[79] glaucoma,[80] and neovascular retinal diseases[81] among others. The AH is a robust source of molecular information for a multitude of ocular conditions, with growing indications for clinical use.

The long-term goal of this study has been to identify and understand the clinical impact of tumor-derived biomarkers in the cfDNA identified in the AH liquid biopsy. This includes diagnosis of RB (*RB1* mutations), the prognosis for response to therapy and likelihood of ocular salvage (SCNAs), pathogenic alterations (SNV) in *RB1*, and TFx as a biomarker to monitor intraocular response to therapy longitudinally (TFx). Over the past several years, we have developed a robust clinical data and specimen biorepository, now with prospective and longitudinal AH samples, from which we continue to identify novel biomarkers that may improve our understanding of the mechanisms of aggressive intraocular tumor behavior. Ultimately, we believe that this research represents a significant step toward a molecular-based, precision medicine approach for children with RB. Continued prospective validation of the tumor-derived molecular biomarkers discussed is needed; this has potential to provide impactful, objective information to clinicians and may not only guide treatment decisions but also lead to new targeted therapies based on the data generated from this and other studies in the future.

## Acknowledgments:

We would like to thank the retinoblastoma cancer patients and their families' participation for providing specimens to the advancement of cancer research. We are grateful to the research support provided by Children's Hospital Los Angeles team RAPIDO: Brianne Brown, Mark Reid, Dilshad Contractor, and Armine Begijanmasihi.

**Funding/Support:**

This work was supported by the National Cancer Institute of the National Institutes of Health (K08CA232344, R01CA282759), the Wright Foundation, Children's Oncology Group/St. Baldrick's Foundation, the Knights Templar Eye Foundation, Hyundai Hope on Wheels, Childhood Eye Cancer Trust, Children's Cancer Research Fund, and the Alex's Lemonade Stand Foundation for Childhood Cancer. Other research support comes from A. Linn Murphree, MD, Chair in Retinoblastoma, the Danhakl Family Foundation, the Berle & Lucy Adams Chair in Cancer Research, the Larry and Celia Moh Foundation, the Institute for Families, Inc, and Children's Hospital Los Angeles, and an unrestricted departmental grant from Research to Prevent Blindness.

## REFERENCES

1. Dimaras H, Corson TW, Cobrinik D, et al. Retinoblastoma. Nat Rev Dis Primers. 2015;1:15021. doi: 10.1038/nrdp.2015.21. [PubMed: 27189421]
2. Rao R, Retinoblastoma Honavar SG. Indian J Pediatr. 2017;84(12):937–944. doi: 10.1007/s12098-017-2395-0. [PubMed: 28620731]
3. Global Retinoblastoma Study GroupThe Global Retinoblastoma Outcome Study: a prospective, cluster-based analysis of 4064 patients from 149 countries. Lancet Glob Health. 2022;10(8):e1128–e1140. doi: 10.1016/S2214-109X(22)00250-9. [PubMed: 35839812]
4. Zhao J, Feng ZX, Wei M, et al. Impact of systemic chemotherapy and delayed enucleation on survival of children with advanced intraocular retinoblastoma. Ophthalmol Retina. 2020;4(6):630–639. doi: 10.1016/j.oret.2020.02.015. [PubMed: 32387053]
5. Ancona-Lezama D, Dalvin LA, Shields CL. Modern treatment of retinoblastoma: a 2020 review. Indian J Ophthalmol. 2020;68(11):2356–2365. doi:10.4103/ijo.IJO_721_20. [PubMed: 33120616]
6. Berry JL, Shah S, Bechtold M, Zolfaghari E, Jubran R, Kim JW. Long-term outcomes of group D retinoblastoma eyes during the intravitreal melphalan era. Pediatr Blood Cancer. 2017;64(12):e26696. doi: 10.1002/pbc.26696.
7. Tomar AS, Finger PT, Gallie B, et al. A multicenter, international collaborative study for American joint committee on cancer staging of retinoblastoma: part II: treatment success and globe salvage. Ophthalmology. 2020;127(12):1733–1746. doi: 10.1016/j.ophtha.2020.05.051. [PubMed: 32526306]

8. Eriksson O, Hagmar B, Ryd W. Effects of fine-needle aspiration and other biopsy procedures on tumor dissemination in mice. Cancer. 1984;54(1):73–78. [PubMed: 6722746]
9. Eide N, Walaas L. Fine-needle aspiration biopsy and other biopsies in suspected intraocular malignant disease: a review. Acta Ophthalmol. 2009;87(6):588–601. doi: 10.1111/j.1755-3768.2009.01637.x. [PubMed: 19719804]
10. Shields JA, Shields CL, Ehya H, Eagle RC Jr, De Potter P. Fine-needle aspiration biopsy of suspected intraocular tumors. The 1992 Urwick Lecture. Ophthalmology. 1993;100(11):1677–1684. [PubMed: 8233394]
11. Karcioglu ZA, Gordon RA, Karcioglu GL. Tumor seeding in ocular fine needle aspiration biopsy. Ophthalmology. 1985;92(12):1763–1767. [PubMed: 4088631]
12. Fung YK, Murphree AL, T'Ang A, Qian J, Hinrichs SH, Benedict WF. Structural evidence for the authenticity of the human retinoblastoma gene. Science. 1987;236(4809):1657–1661. [PubMed: 2885916]
13. Corson TW, Gallie BL. One hit, two hits, three hits, more? Genomic changes in the development of retinoblastoma. Genes Chromosomes Cancer. 2007;46(7):617–634. doi: 10.1002/gcc.20457. [PubMed: 17437278]
14. Do K, O'Sullivan Coyne G, Chen AP. An overview of the NCI precision medicine trials-NCI MATCH and MPACT. Chin Clin Oncol. 2015;4(3):31. doi: 10.3978/j.issn.2304-3865.2015.08.01. [PubMed: 26408298]
15. Children successfully MATCHed to therapies. Cancer Discov. 2019;9(7):OF3. doi: 10.1158/2159-8290.CD-NB2019-059.
16. Berry JL, Xu L, Murphree AL, et al. Potential of aqueous humor as a surrogate tumor biopsy for retinoblastoma. JAMA Ophthalmol. 2017;135(11):1221–1230. doi: 10.1001/jamaophthalmol.2017.4097. [PubMed: 29049475]
17. Berry JL, Cobrinik D, Hicks J. Potential of aqueous humor as a surrogate tumor biopsy for retinoblastoma—reply. JAMA Ophthalmol. 2018;136(5):598. doi: 10.1001/jamaophthalmol.2018.0395. [PubMed: 29566117]
18. Berry JL, Xu L, Kooi I, et al. Genomic cfDNA analysis of aqueous humor in retinoblastoma predicts eye salvage: the surrogate tumor biopsy for retinoblastoma. Mol Cancer Res. 2018;16(11):1701–1712. doi: 10.1158/1541-7786.MCR-18-0369. [PubMed: 30061186]
19. Kim ME, Polski A, Xu L, et al. Comprehensive somatic copy number analysis using aqueous humor liquid biopsy for retinoblastoma. Cancers (Basel). 2021;13(13):3340. doi: 10.3390/cancers13133340. [PubMed: 34283049]
20. Xu L, Shen L, Polski A, et al. Simultaneous identification of clinically relevant RB1 mutations and copy number alterations in aqueous humor of retinoblastoma eyes. Ophthalmic Genet. 2020;41(6):526–532. doi: 10.1080/13816810.2020.1799417. [PubMed: 32799607]
21. Xu L, Polski A, Prabakar RK, et al. Chromosome 6p amplification in aqueous humor cell-free DNA is a prognostic biomarker for retinoblastoma ocular survival. Mol Cancer Res. 2020;18(8):1166–1175. doi: 10.1158/1541-7786.MCR-19-1262. [PubMed: 32434859]
22. Xu L, Kim ME, Polski A, et al. Establishing the clinical utility of ctDNA analysis for diagnosis, prognosis, and treatment monitoring of retinoblastoma: the aqueous humor liquid biopsy. Cancers (Basel). 2021;13(6):1282. doi: 10.3390/cancers13061282. [PubMed: 33805776]
23. Polski A, Xu L, Prabakar RK, et al. Cell-free DNA tumor fraction in the aqueous humor is associated with therapeutic response in retinoblastoma patients. Transl Vis Sci Technol. 2020;9(10):30. doi: 10.1167/tvst.9.10.30.
24. Li HT, Xu L, Weisenberger DJ, et al. Characterizing DNA methylation signatures of retinoblastoma using aqueous humor liquid biopsy. Nat Commun. 2022;13(1):5523. doi: 10.1038/s41467-022-33248-2. [PubMed: 36130950]
25. Liu J, Ottaviani D, Sefta M, et al. A high-risk retinoblastoma subtype with stemness features, dedifferentiated cone states and neuronal/ganglion cell gene expression. Nat Commun. 2021;12(1):5578. doi: 10.1038/s41467-021-25792-0. [PubMed: 34552068]
26. Wong EY, Xu L, Shen L, et al. Inter-eye genomic heterogeneity in bilateral retinoblastoma via aqueous humor liquid biopsy. NPJ Precis Oncol. 2021;5(1):73. [PubMed: 34316014]

27. Berry JL, Xu L, Polski A, et al. Aqueous humor is superior to blood as a liquid biopsy for retinoblastoma. Ophthalmology. 2020;127(4):552–554. doi: 10.1016/j.ophtha.2019.10.026. [PubMed: 31767439]
28. Ghose N, Kaliki S. Liquid biopsy in retinoblastoma: a review. Semin Ophthalmol. 2022;37(7–8):813–819. doi: 10.1080/08820538.2022.2078165. [PubMed: 35604935]
29. Gerrish A, Stone E, Clokie S, et al. Non-invasive diagnosis of retinoblastoma using cell-free DNA from aqueous humour. Br J Ophthalmol. 2019;103:721–724. doi: 10.1136/bjophthalmol-2018-313005. [PubMed: 30745306]
30. Le Gall J, Dehainault C, Benoist C, et al. Highly sensitive detection method of retinoblastoma genetic predisposition and biomarkers. J Mol Diagn. 2021;23(12):1714–1721. doi: 10.1016/j.jmoldx.2021.08.014. [PubMed: 34656762]
31. Raval V, Racher H, Wrenn J, Singh AD. Aqueous humor as a surrogate biomarker for retinoblastoma tumor tissue. J AAPOS. 2022;26(3) 137.e1–137.e5. doi: 10.1016/j.jaapos.2022.03.005.
32. Gerrish A, Jenkinson H, Cole T. The impact of cell-free DNA analysis on the management of retinoblastoma. Cancers (Basel).. 2021;13(7):1570. doi: 10.3390/cancers13071570. [PubMed: 33805427]
33. Alfaar AS, Chantada G, Qaddoumi I. Survivin is high in retinoblastoma, but what lies beneath? J AAPOS. 2018;22(6):482. doi: 10.1016/j.jaapos.2017.02.021.
34. Liu W, Luo Y, Dai J, et al. Monitoring retinoblastoma by machine learning of aqueous humor metabolic fingerprinting. Small Methods. 2022;6(1):e2101220. doi: 10.1002/smtd.202101220. [PubMed: 35041286]
35. Busch MA, Haase A, Miroschnikov N, et al. TFF1 in aqueous humor—a potential new biomarker for retinoblastoma. Cancers (Basel). 2022;14(3):677. doi: 10.3390/cancers14030677. [PubMed: 35158945]
36. Cancellieri F, Peter VG, Quinodoz M, Stathopoulos C, Munier FL, Rivolta C. Genetic bases of retinoblastoma from liquid biopsies. Invest Ophth Vis Sci. 2022;63(7):503–A0080.
37. Murphree AL. Intraocular retinoblastoma: the case for a new group classification. Ophthalmol Clin North Am. 2005;18(1):41–53. [PubMed: 15763190]
38. Berry JL, Jubran R, Kim JW, et al. Long-term outcomes of Group D eyes in bilateral retinoblastoma patients treated with chemoreduction and low-dose IMRT salvage. Pediatr Blood Cancer. 2013;60(4):688–693. doi: 10.1002/pbc.24303. [PubMed: 22997170]
39. Shields CL, Shields JA. Intra-arterial chemotherapy for retinoblastoma. JAMA Ophthalmol. 2016;134(10):1201. doi: 10.1001/jamaophthalmol.2016.2712.
40. Kim ME, Xu L, Prabakar RK, et al. Aqueous humor as a liquid biopsy for retinoblastoma: clear corneal paracentesis and genomic analysis. J Vis Exp. 2021(175). doi: 10.3791/62939.
41. Baslan T, Kendall J, Rodgers L, et al. Genome-wide copy number analysis of single cells. Nat Protoc. 2012;7(6):1024–1041. doi: 10.1038/nprot.2012.039. [PubMed: 22555242]
42. Baslan T, Kendall J, Rodgers L, et al. Corrigendum: genome-wide copy number analysis of single cells. Nat Protoc. 2016;11(3):616. doi: 10.1038/nprot0316.616b.
43. Adalsteinsson VA, Ha G, Freeman SS, et al. Scalable whole-exome sequencing of cell-free DNA reveals high concordance with metastatic tumors. Nat Commun. 2017;8(1):1324. doi: 10.1038/s41467-017-00965-y. [PubMed: 29109393]
44. Choudhury AD, Werner L, Francini E, et al. Tumor fraction in cell-free DNA as a biomarker in prostate cancer. JCI Insight. 2018;3(21):e122109. doi: 10.1172/jci.insight.122109. [PubMed: 30385733]
45. Berry JL, Munier FL, Gallie BL, et al. Response criteria for intraocular retinoblastoma: RB-RECIST. Pediatr Blood Cancer. 2021;68(5):e28964. doi: 10.1002/pbc.28964. [PubMed: 33624399]
46. Linn Murphree A. Intraocular retinoblastoma: the case for a new group classification. Ophthalmol Clin North Am. 2005;18(1):41–53 viii. doi: 10.1016/j.ohc.2004.11.003. [PubMed: 15763190]
47. Mallipatna A. AJCC Cancer Staging Manual. 8th ed. Springer; 2017.

48. Reichert ZR, Morgan TM, Li G, et al. Prognostic value of plasma circulating tumor DNA fraction across four common cancer types: a real-world outcomes study. Ann Oncol. 2023;34(1):111–120. doi: 10.1016/j.annonc.2022.09.163. [PubMed: 36208697]
49. Elazezy M, Joosse SA. Techniques of using circulating tumor DNA as a liquid biopsy component in cancer management. Comput Struct Biotechnol J. 2018;16:370–378. doi: 10.1016/j.csbj.2018.10.002. [PubMed: 30364656]
50. Rushlow DE, Mol BM, Kennett JY, et al. Characterisation of retinoblastomas without RB1 mutations: genomic, gene expression, and clinical studies. Lancet Oncol. 2013;14(4):327–334. doi: 10.1016/S1470-2045(13)70045-7. [PubMed: 23498719]
51. Afshar AR, Pekmezci M, Bloomer MM, et al. Next-generation sequencing of retinoblastoma identifies pathogenic alterations beyond RB1 inactivation that correlate with aggressive histopathologic features. Ophthalmology. 2020;127(6):804–813. doi: 10.1016/j.ophtha.2019.12.005. [PubMed: 32139107]
52. Schwermer M, Hiber M, Dreesmann S, et al. Comprehensive characterization of RB1 mutant and MYCN amplified retinoblastoma cell lines. Exp Cell Res. 2019;375(2):92–99. doi: 10.1016/j.yexcr.2018.12.018. [PubMed: 30584916]
53. Francis JH, Richards AL, Mandelker DL, et al. Molecular changes in retinoblastoma beyond RB1: findings from next-generation sequencing. Cancers (Basel).. 2021;13(1):149. doi: 10.3390/cancers13010149. [PubMed: 33466343]
54. Polski A, Xu L, Prabakar RK, et al. Variability in retinoblastoma genome stability is driven by age and not heritability. Genes Chromosomes Cancer. 2020;59(10):584–590. doi: 10.1002/gcc.22859. [PubMed: 32390242]
55. Martelotto LG, Baslan T, Kendall J, et al. Whole-genome single-cell copy number profiling from formalin-fixed paraffin-embedded samples. Nat Med. 2017;23(3):376–385. doi: 10.1038/nm.4279. [PubMed: 28165479]
56. Ghiam BK, Xu L, Berry JL. Aqueous humor markers in retinoblastoma, a review. Transl Vis Sci Technol. 2019;8(2):13. doi: 10.1167/tvst.8.2.13.
57. Mol BM, Massink MP, van der Hout AH, et al. High-resolution SNP array profiling identifies variability in retinoblastoma genome stability. Genes Chromosomes Cancer. 2014;53(1):1–14. doi: 10.1002/gcc.22111. [PubMed: 24249257]
58. Stålhammar G, Yeung A, Mendoza P, Dubovy SR, William Harbour J, Grossniklaus HE. Gain of chromosome 6p correlates with severe anaplasia, cellular hyperchromasia, and extraocular spread of retinoblastoma. Ophthalmol Sci. 2022;2(1):100089. doi: 10.1016/j.xops.2021.100089. [PubMed: 36246172]
59. Santos GC, Zielenska M, Prasad M, Squire JA. Chromosome 6p amplification and cancer progression. J Clin Pathol. 2007;60(1):1–7. doi: 10.1136/jcp.2005.034389. [PubMed: 16790693]
60. Chen D, Gallie BL, Squire JA. Minimal regions of chromosomal imbalance in retinoblastoma detected by comparative genomic hybridization. Cancer Genet Cytogenet. 2001;129(1):57–63. doi: 10.1016/s0165-4608(01)00427-7. [PubMed: 11520568]
61. Kooi IE, Mol BM, Massink MP, et al. A meta-analysis of retinoblastoma copy numbers refines the list of possible driver genes involved in tumor progression. PLoS One. 2016;11(4):e0153323. doi: 10.1371/journal.pone.0153323. [PubMed: 27115612]
62. Grasemann C, Gratias S, Stephan H, et al. Gains and overexpression identify DEK and E2F3 as targets of chromosome 6p gains in retinoblastoma. Oncogene. 2005;24(42):6441–6449. doi: 10.1038/sj.onc.1208792. [PubMed: 16007192]
63. Kooi IE, Mol BM, Massink MP, et al. Somatic genomic alterations in retinoblastoma beyond RB1 are rare and limited to copy number changes. Sci Rep.. 2016;6:25264. doi: 10.1038/srep25264. [PubMed: 27126562]
64. Devarajan B, Prakash L, Kannan TR, et al. Targeted next generation sequencing of RB1 gene for the molecular diagnosis of retinoblastoma. BMC Cancer. 2015;15:320. doi: 10.1186/s12885-015-1340-8. [PubMed: 25928201]
65. Greger V, Debus N, Lohmann D, Höpping W, Passarge E, Horsthemke B. Frequency and parental origin of hypermethylated RB1 alleles in retinoblastoma. Hum Genet. 1994;94(5):491–496. [PubMed: 7959682]

66. Raizis AM, Racher HM, Foucal A, Dimaras H, Gallie BL, George PM. DNA hypermethylation/boundary control loss identified in retinoblastomas associated with genetic and epigenetic inactivation of the *RB1* gene promoter. Epigenetics. 2021;16(9):940–954. [PubMed: 33258708]

67. van den Bosch T, van Beek JG, Vaarwater J, et al. Higher percentage of FISH-determined monosomy 3 and 8q amplification in uveal melanoma cells relate to poor patient prognosis. Invest Ophthalmol Vis Sci. 2012;53(6):2668–2674. doi: 10.1167/iovs.11-8697. [PubMed: 22427574]

68. Jager MJ, Brouwer NJ, Esmaeli B. The cancer genome atlas project: an integrated molecular view of uveal melanoma. Ophthalmology. 2018;125(8):1139–1142. doi: 10.1016/j.ophtha.2018.03.011. [PubMed: 30032793]

69. Christodoulou E, Yellapantula V, O'Halloran K, et al. Combined low-pass whole genome and targeted sequencing in liquid biopsies for pediatric solid tumors. NPJ Precis Oncol. 2023;7(1):21. doi: 10.1038/s41698-023-00357-0. [PubMed: 36805676]

70. Murciano-Goroff YR, Drilon A, Stadler ZK. The NCI-MATCH: a national, collaborative precision oncology trial for diverse tumor histologies. Cancer Cell. 2021;39(1):22–24. doi: 10.1016/j.ccell.2020.12.021. [PubMed: 33434511]

71. Flaherty KT, Gray RJ, Chen AP, et al. Molecular landscape and actionable alterations in a genomically guided cancer clinical trial: National Cancer Institute Molecular Analysis for Therapy Choice (NCI-MATCH). J Clin Oncol. 2020;38(33):3883–3894. doi: 10.1200/JCO.19.03010. [PubMed: 33048619]

72. Luo Y, Xu M, Yang L, et al. Correlating somatic copy number alteration in aqueous humour cfDNA with chemotherapy history, eye salvage and pathological features in retinoblastoma. Br J Ophthalmol. 2024;108(3):449–456. doi: 10.1136/bjo-2022-322866. [PubMed: 36931696]

73. Zeng Q, Wang S, Tan J, Chen L, Wang J. The methylation level of TFAP2A is a potential diagnostic biomarker for retinoblastoma: an analytical validation study. PeerJ. 2021;9:e10830. doi:10.7717/peerj.10830. [PubMed: 33717678]

74. Galardi A, Stathopoulos C, Colletti M, et al. Proteomics of aqueous humor as a source of disease biomarkers in retinoblastoma. Int J Mol Sci. 2022;23(21):13458. doi: 10.3390/ijms232113458. [PubMed: 36362243]

75. Peng CC, Im D, Sirivolu S, et al. Single vesicle analysis of aqueous humor in pediatric ocular diseases reveals eye specific CD63-dominant subpopulations. J Extracell Biol. 2022;1(4):e36. doi: 10.1002/jex2.36. [PubMed: 36339649]

76. Im DH, Peng CC, Xu L, et al. Potential of aqueous humor as a liquid biopsy for uveal melanoma. Int J Mol Sci. 2022;23(11):6226. doi: 10.3390/ijms23116226. [PubMed: 35682905]

77. Wierenga APA, Cao J, Mouthaan H, et al. Aqueous humor biomarkers identify three prognostic groups in uveal melanoma. Invest Ophthalmol Vis Sci. 2019;60(14):4740–4747. doi: 10.1167/iovs.19-28309. [PubMed: 31731294]

78. Demirci H, Rao RC, Elner VM, et al. Aqueous humor-derived MYD88 L265P mutation analysis in vitreoretinal lymphoma: a potential less invasive method for diagnosis and treatment response assessment. Ophthalmol Retina. 2023;7(2):189–195. doi: 10.1016/j.oret.2022.08.005. [PubMed: 35952929]

79. Kang GY, Bang JY, Choi AJ, et al. Exosomal proteins in the aqueous humor as novel biomarkers in patients with neovascular age-related macular degeneration. J Proteome Res. 2014;13(2):581–595. doi: 10.1021/pr400751k. [PubMed: 24400796]

80. Sharma S, Bollinger KE, Kodeboyina SK, et al. Proteomic alterations in aqueous humor from patients with primary open angle glaucoma. Invest Ophthalmol Vis Sci. 2018;59(6):2635–2643. doi: 10.1167/iovs.17-23434. [PubMed: 29847670]

81. Hsiao YP, Chen C, Lee CM, et al. Differences in the quantity and composition of extracellular vesicles in the aqueous humor of patients with retinal neovascular diseases. Diagnostics (Basel). 2021;11(7):1276. doi: 10.3390/diagnostics11071276. [PubMed: 34359359]

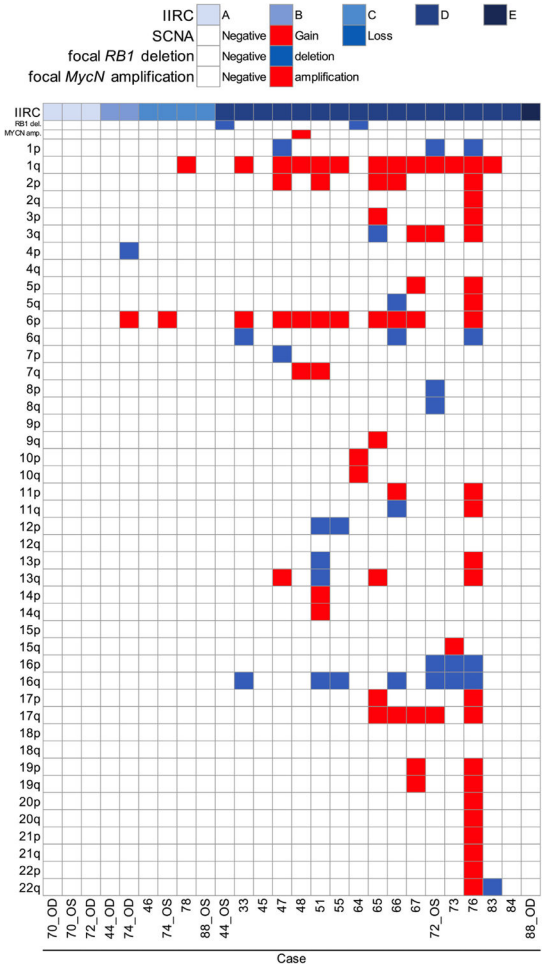


**FIGURE 1.**

Genome-wide somatic copy number alterations (SCNAs) in the aqueous humor (AH) of retinoblastoma eyes. Schematic heatmap of SCNAs identified via an AH liquid biopsy at diagnosis. IIRC = International Intraocular Retinoblastoma Classification.

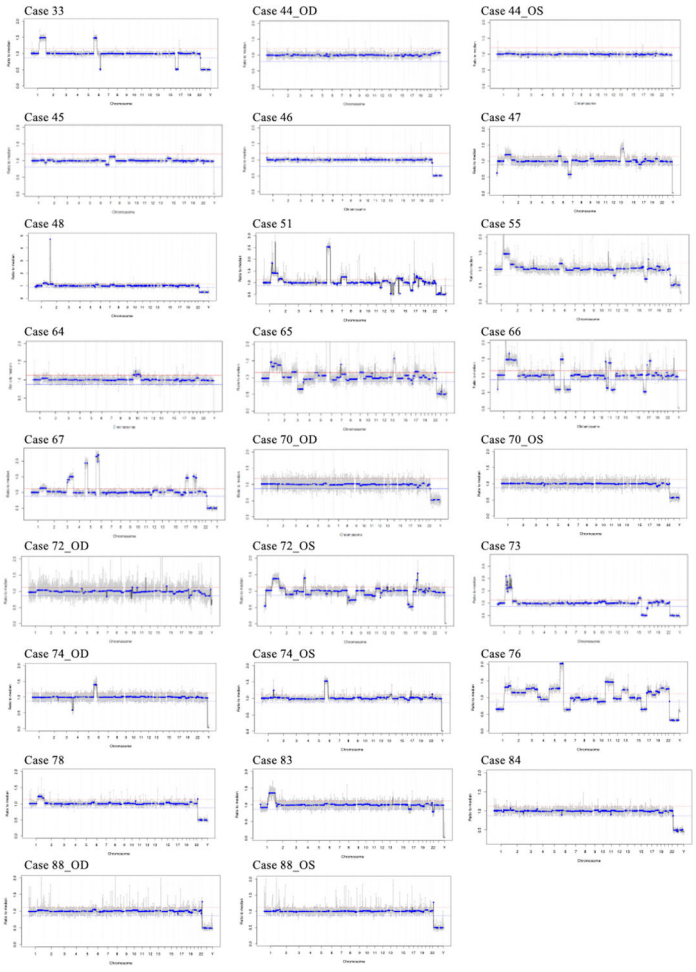


**FIGURE 2.**

Retinoblastoma genomic profiles from the aqueous humor liquid biopsy. The diagnostic genomic profile from each eye is shown; the *x*-axis shows the chromosomal location, the *y*-axis demonstrates the copy number values that are recorded as ratios to the median (relative to a baseline human genome), with values ≤0.87 representing copy number losses and values ≥1.15 representing copy number gains equal to 20% deflection from the human genome (red line).

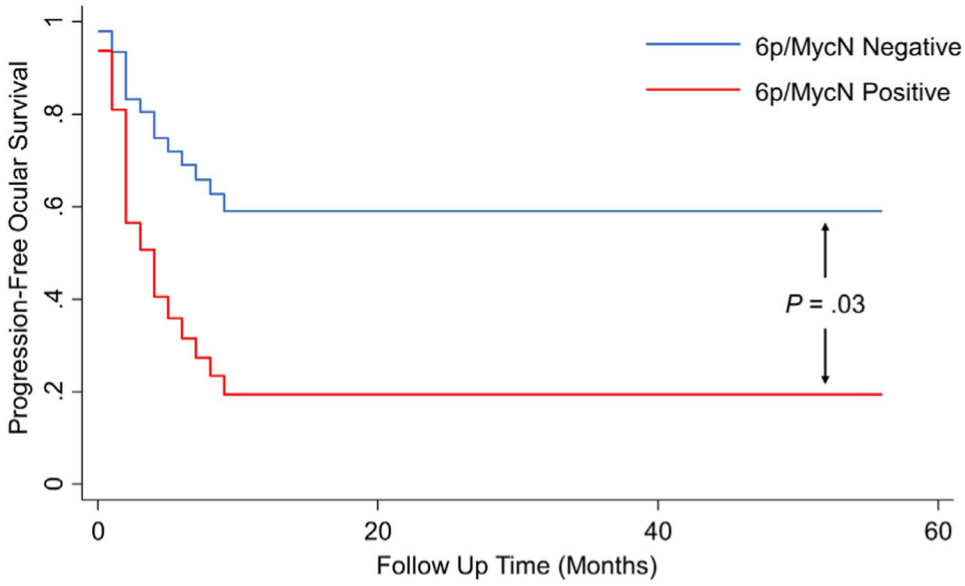


**FIGURE 3.**

Progression-free ocular survival over time by biomarker status. Aqueous humor with either 6p gain or MycN amplification (red line) shows reduced progression-free ocular survival rates over time compared with noncarriers (blue line).

**TABLE 1.**

Clinical Demographics, Diagnostic Clinical Features, and Therapeutic Courses for Each Study Participant

| Case ID | Eye | Sex | Age at DX (mo) | Laterality | IIRC (TNM) | Family History of RB? | Vitreous Seeding at DX | Initial Treatment | Seeding Recurrence? | Retinal Recurrence? | Total Sample Number | Time to Enucleation (mo) | Follow-up From DX (mo) |
|---|---|---|---|---|---|---|---|---|---|---|---|---|---|
| **33** | OS | M | 22 | U | D (CT2B) | Negative | Sphere | IAC | Yes | No | 5 | 5 | 47 |
| **44** | OD | M | 4 | B | B (CT1B) | Negative | None | IVC | No | No | 2 | n/a | 55 |
| — | OS | M | 4 | B | D (CT2B) | Negative | Dust | IVC | Yes | Yes | 11 | n/a | 55 |
| **45** | OD | F | 8 | U | D (CT2B) | Negative | None | IVC | No | No | 1 | n/a | 56 |
| **46** | OS | M | 5 | U | C (CT2A) | Negative | None | IVC | No | No | 2 | n/a | 37 |
| **47** | OD | F | 15 | U | D (CT2B) | Negative | Sphere | IVC | Yes | No | 4 | n/a | 46 |
| **48** | OD | M | 18 | U | D (CT2B) | Negative | Cloud | IAC | No | Yes | 1 | 1 | 47 |
| **51** | OD | M | 30 | U | D (CT2B) | Negative | Dust | IAC | No | No | 3 | n/a | 41 |
| **55** | OS | M | 24 | U | D (CT2B) | Negative | Sphere | IAC | Yes | No | 3 | 5 | 38 |
| **64** | OD | F | 15 | B | D (CT2B) | Negative | Sphere | IVC | No | No | 1 | n/a | 36 |
| **65** | OS | M | 24 | U | D (CT2B) | Negative | Cloud, sphere | PE | n/a | n/a | 2 | 0 | 34 |
| **66** | OS | F | 24 | B | D (CT2B) | Negative | Cloud | IAC | Yes | No | 5 | 9 | 35 |
| **67** | OS | M | 24 | U | D (CT2B) | Negative | Dust | IAC | No | Yes | 2 | 2 | 29 |
| **70** | OD | M | 2 | B | A (CT1A) | Positive | None | Laser | No | No | 1 | n/a | 33 |
| — | OS | M | 2 | B | A (CT1A) | Positive | None | Laser | No | No | 1 | n/a | 33 |
| **72** | OD | F | 27 | B | A (CT1A) | Positive | None | IVC | No | No | 1 | n/a | 24 |
| — | OS | F | 27 | B | D (CT2B) | Positive | Cloud | IVC | No | Yes | 1 | 7 | 24 |
| **73** | OS | M | 35 | U | D (CT2B) | Negative | Cloud | IVC | Yes | No | 16 | n/a | 22 |
| **74** | OD | F | 4 | B | B (CT1B) | Negative | None | IVC | No | Yes | 4 | n/a | 21 |
| — | OS | F | 4 | B | C (CT2B) | Negative | Subretinal | IVC | No | No | 3 | n/a | 21 |
| **76** | OS | M | 46 | U | D (CT2B) | Negative | Subretinal | IVC | Yes | No | 7 | n/a | 21 |
| **78** | OS | M | 4 | U | C (CT2B) | Negative | Subretinal | IVC | No | No | 3 | n/a | 21 |
| **83** | OS | F | 8 | U | D (CT2B) | Negative | Sphere | Bridge IAC | No | No | 1 | n/a | 18 |
| **84** | OD | M | 6 | U | D (CT2B) | Negative | Dust | IVC | Yes | No | 4 | n/a | 16 |
| **88** | OD | M | 5 | B | E (CT3C) | Negative | Dust | IVC | Yes | No | 2 | n/a | 12 |
| — | OS | M | 5 | B | C (CT2B) | Negative | Sphere | IVC | Yes | No | 3 | n/a | 12 |

B = bilateral, DX = diagnosis, IAC = intra-arterial chemotherapy, IIRC = International Intraocular Retinoblastoma Classification, IVC = systemic intravenous chemotherapy, n/a = not applicable, PE = primary enucleation, RB = retinoblastoma, TNM = tumor, nodes, metastases, U = unilateral.

**TABLE 2.**

Pathogenic *RB1* Variants and Cell-Free DNA Concentrations for All 26 Diagnostic Aqueous Humor Samples

| Case ID_Eye if Bilateral | gDNA *RB1* Variant | AH *RB1* Variants | % VAF | Total Reads, Altered Reads | 95% CI | dsDNA (ng/μL) |
|---|---|---|---|---|---|---|
| **33** | Negative | c.2325+ 1G>A | 99.7 | 957, 954 | 99.0–100.0 | 3.4 |
| **44_OD** | c.1666C>T | c.1666C>T | 67.2 | 64, 43 | 53.6–80.8 | 1.2 |
| **44_OS** | c.1666C>T | c.1666C>T | 98.7 | 947, 935 | 97.4–99.7 | 2.3 |
| — | — | *RB1* gene deletion | — | — | — | — |
| **45** | Negative | c.1422–1G>A | 97.9 | 330,323 | 95.5–100.0 | 0.6 |
| **46** | Negative | c.1363C>T | 99.4 | 359,357 | 93.3–98.1 | 0.5 |
| **47** | Negative | c.958C>T | 93.5 | 31, 29 | 73.1–99.7 | 3.0 |
| **48** | Negative | ND | ND | ND | — | 4.1 |
| **51** | Negative | Loss of 13q | — | — | — | n/a |
| **55** | Negative | c.869dup | 43.3 | 30, 13 | 32.3–72.4 | n/a |
| — | — | c.1215+1G>A | 40.8 | 71, 29 | 33.0–58.0 | n/a |
| **64** | Heterozygous deletion of exons 24–27 | *RB1* gene deletion | — | — | — | n/a |
| **65** | Negative | c.1589_1590del | 66.7 | 6, 4 | 20.6–98.3 | 24.0 |
| — | — | c.2330dup | 33.3 | 6, 2 | 3.9–76.2 | 24.0 |
| **66** | c.1362 C>G | c.380G>T | 50.0 | 42, 21 | 38.6–69.2 | 46.4 |
| — | — | c.1362C>G | 30.5 | 59, 18 | 20.2–47.4 | 46.4 |
| **67** | Negative | c.1028_1029del | 40.4 | 104,42 | 36.0–53.0 | 0.5 |
| — | — | c.1794_1801dup | 39.6 | 159,63 | 39.3–49.7 | 0.5 |
| **70_OD** | c.607+ 1G>C | ND | ND | ND | — | ND |
| **70_OS** | c.607+ 1G>C | ND | ND | ND | — | 0.5 |
| **72_OD** | c.1399C>T | ND | ND | ND | — | ND |
| **72_OS** | c.1399C>T | c.571G >A | 100 | 24, 24 | — | 56.6 |
| **73** | Negative | c.1333–5_1333del | 97.8 | 89, 87 | 87.6–97.2 | 27.8 |
| **74_OD** | c.1215+1G >A | ND | ND | ND | — | 1.1 |
| **74_OS** | c.1215+1G >A | c.1215+1G>A | 100 | 42, 42 | — | 1.5 |
| **76** | Negative | c.182_183del | 44.6 | 56, 25 | 30.0–53.9 | 0.1 |
| — | — | c.1072C>T | 42.9 | 35, 15 | 26.1–64.8 | 0.1 |
| — | — | c.751C >T | 97.5 | 237, 231 | 93.0–97.4 | 0.1 |

| Case ID_Eye if Bilateral | gDNA *RB1* Variant | AH *RB1* Variants | % VAF | Total Reads, Altered Reads | 95% CI | dsDNA (ng/μL) |
|---|---|---|---|---|---|---|
| **78** | c.958C>T | c.958C >T | 97.6 | 42, 41 | 90.1–98.8 | 0.4 |
| **83** | Negative | ND | ND | ND | — | 0.5 |
| **84** | Negative | ND | ND | ND | — | 0.1 |
| **88_OD** | c.1996dup | c.1996dup | 100 | 63, 63 | — | 0.6 |
| **88_OS** | c.1996dup | c.1996dup | 93.2 | 74, 69 | 87.3–96.3 | 0.3 |

AH = aqueous humor, dsDNA = double-stranded DNA; gDNA = genomic DNA, n/a = not available, ND = not detected, VAF = variant allele frequency.

**TABLE 3.**

Somatic Copy Number Alterations (SCNAs) and Tumor Fraction (TFx) Values for All 26 Diagnostic Aqueous Humor Samples

| Case ID_Eye if Bilateral | DX TFx (%) | 6p Amplification | Ratio to Median 6p | Other RB SCNAs[a] | Whole Genome Instability |
|---|---|---|---|---|---|
| **33** | 97.0 | Approximately 1 copy gain | 1.48 | Gain of 1q, loss of 16q | Positive |
| **44_OD** | 4.0 | Negative | 1.02 | — | Negative |
| **44_OS** | 3.2 | Negative | 1.01 | *RB1* gene deletion | Negative |
| **45** | 11.8 | Negative | 1.02 | — | Negative |
| **46** | 6.7 | Negative | 1.01 | — | Negative |
| **47** | 22.7 | Approximately 1 copy gain | 1.14 | Gain of 1q, 2p | Positive |
| **48** | 11.2 | Approximately 1 copy gain | 1.14 | Focal *MycN* amplification, gain of 1q | Positive |
| **51** | 41.9 | Multicopy gain | 2.52 | Gain of 1q, 2p; loss of 13q, 16q | Positive |
| **55** | 46.4 | Approximately 1 copy gain | 1.18 | Gain of 1q, loss of 16q | Positive |
| **64** | 28.4 | Negative | 0.99 | *RB1* gene deletion | Negative |
| **65** | 39.0 | Multicopy gain | 2.87 | Gain of 1q, 2p | Positive |
| **66** | 87.0 | Approximately 1 copy gain | 1.51 | Gain of 1q, 2p, loss of 16q | Positive |
| **67** | 45.9 | Multicopy gain | 2.15 | Gain of 1q | Positive |
| **70_OD** | 11.1 | Negative | 1.03 | — | Negative |
| **70_OS** | 0 | Negative | 1.01 | — | Negative |
| **72_OD** | 31.0 | Negative | 1.02 | — | Negative |
| **72_OS** | 72.1 | Negative | 1.00 | Gain of 1q, loss of 16q | Positive |
| **73** | 41.8 | Negative | 1.04 | Focal *MDM4* amplification, gain of 1q, loss of 16q | Positive |
| **74_OD** | 39.5 | Approximately 1 copy gain | 1.40 | — | Positive |
| **74_OS** | 36.1 | Approximately 1 copy gain | 1.52 | — | Positive |
| **76** | 64.2 | Multicopy gain | 2.02 | Gain of 1q, 2p, loss of 16q | Positive |
| **78** | 13.6 | Negative | 1.04 | Gain of 1q | Positive |
| **83** | 24.9 | Negative | 1.04 | Gain of 1q | Positive |
| **84** | 5.3 | Negative | 1.01 | — | Negative |
| **88_OD** | 5.4 | Negative | 1.05 | — | Negative |
| **88_OS** | 7.2 | Negative | 1.01 | — | Negative |

DX = diagnostic, RB = retinoblastoma.

[a]Definition of RB SCNAs: gain of 1q, 2p, 6p; loss of 13q, 16q, focal amplifications of *MycN* and *MDM4*, as well as focal *RB1* gene deletions are reported.

**TABLE 4.**

Longitudinal Tumor Fraction (TFx) Values and Corresponding Clinical Information for All Patients With Diagnostic Aqueous Humor Tumor Fraction Values Greater Than 10% and 2 or More Samples

| Case ID_Eye if Bilateral | Sample Timing | Time From Last Sample (wk) | TFx (%) | Therapeutic Response |
|---|---|---|---|---|
| 33 | *DX* | — | 97.0 | Baseline examination |
| | IVitC 1 | 11 | 94.0 | Progressed |
| | IVitC 2 | 2 | 90.7 | Regressed |
| | IVitC 3 | 4 | 97.4 | Regressed |
| | SE | 3 | 94.0 | Progressed |
| 47 | *DX* | — | 22.7 | Baseline examination |
| | IVitC 1 | 25 | 6.2 | Progressed |
| | IVitC 2 | 2 | 5.5 | Progressed |
| | IVitC 3 | 2 | 2.0 | Regressed |
| 51 | *DX* | — | 41.9 | Baseline examination |
| | IAC end | 17 | 5.4 | Regressed |
| | END | 45 | a11.1 | Regressed |
| 55 | DX | — | 46.4 | Baseline examination |
| | IVitC 1 | 8 | 46.8 | Regressed |
| | SE | 4 | 47.6 | Progressed |
| 66 | *DX* | — | 87.0 | Baseline examination |
| | IVitC 1 | 4 | 99.5 | Progressed |
| | IVitC 2 | 5 | 93.1 | Regressed |
| | IVitC 3 | 4 | 63.4 | Regressed |
| | IVitC 4 | 4 | 24.6 | Progressed |
| 67 | *DX* | — | 45.9 | Baseline examination |
| | SE | 4 | 3.1 | Progressed |
| 73 | *DX* | — | 41.8 | Baseline examination |
| | IVitC 1 | 9 | 39.3 | Progressed |
| | IVitC 2 | 3 | 40.4 | Regressed |
| | IVitC 3 | 5 | 46.5 | Regressed |
| | IVitC 4 | 4 | 39.6 | Regressed |

| Case ID_Eye if Bilateral | Sample Timing | Time From Last Sample (wk) | TFx (%) | Therapeutic Response |
|---|---|---|---|---|
| | IVitC 5/IVC end | 3 | 43.7 | Regressed |
| | IVitC 6[a] | 4 | 55.6 | Progressed |
| | IVitC 7 | 2 | 6.0 | Progressed |
| | IVitC 8 | 1 | 9.9 | Regressed |
| | IVitC 9 | 2 | 27.0 | Regressed |
| | IVitC 10 | 1 | 8.5 | Regressed |
| | IVitC 11 | 2 | 9.9 | Regressed |
| | IVitC 12 | 2 | 5.7 | Regressed |
| | IViatC 13 | 1 | 5.3 | Regressed |
| | IVitC 14 | 2 | 0.6 | Regressed |
| | IVitC 15 | 2 | 0.0 | Regressed |
| 74_OD | *DX* | — | 39.5 | Baseline examination |
| | IVC end | 5 | 1.7 | Regressed |
| | REC 1 | 4 | 0.0 | Progressed |
| | END | 9 | 0.0 | Regressed |
| 74_OS | *DX* | — | 36.1 | Baseline examination |
| | IVC End | 5 | 7.6 | Regressed |
| 76 | *DX* | — | 64.2 | Baseline examination |
| | IVC End | 4 | 2.3 | Regressed |
| | IVitC 1 | 7 | 5.7 | Progressed |
| | IVitC 2 | 3 | 8.8 | Regressed |
| | IVitC 3 | 4 | 2.7 | Regressed |
| | IVitC 4 | 2 | 0.0 | Regressed |
| | IVitC 5 | 2 | 4.0 | Regressed |
| 78 | *DX* | — | 13.6 | Baseline examination |
| | IVC end | 4 | 2.4 | Regressed |
| | END | 21 | 3.8 | Regressed |
| 76 | *DX* | — | 64.2 | Baseline examination |
| | IVC end | 4 | 2.3 | Regressed |
| | IVitC 1 | 7 | 5.7 | Progressed |
| | IVitC 2 | 3 | 8.8 | Regressed |

| Case ID_Eye if Bilateral | Sample Timing | Time From Last Sample (wk) | TFx (%) | Therapeutic Response |
|---|---|---|---|---|
| | IVitC 3 | 4 | 2.7 | Regressed |
| | IVitC 4 | 2 | 0.0 | Regressed |
| | IVitC 5 | 2 | 4.0 | Regressed |
| 78 | *DX* | — | 13.6 | Baseline examination |
| | IVC end | 4 | 2.4 | Regressed |
| | END | 21 | 3.8 | Regressed |

DX = diagnostic, END = end of treatment, IAC = intra-arterial chemotherapy, IVC = systemic intravenous chemotherapy, IVitC = intravitreal chemotherapy, REC = retinal recurrence, SE = secondary enucleation, TFx = tumor fraction.

[a]Initiation of topoisomerase and melphalan combination intravitreal chemotherapy.